Desalination and Water Treatment
www.deswater.com

doi: 10.5004/dwt.2019.24387

164 (2019) 185–191
October

^{60}Co-traces sorption in the presence of Fe(III)-^{59}Fe in aqueous solutions by banana husk ash obtained through solution combustion process at different temperatures

H. López-González[a], M.T. Olguín[a,*], S. Bulbulian[b]

[a]*Instituto Nacional de Investigaciones Nucleares, Carretera México-Toluca S/N, La Marquesa, Ocoyoacac Estado de México, C. P. 52750, México, email: teresa.olguin@inin.gob.mx (M.T. Olguín)*
[b]*Centro de Ciencias Aplicadas y Desarrollo Tecnológico, Cd. Universitaria A. P. 70-186, C. P. 04510, Ciudad de México, México*

Received 18 February 2019; Accepted 10 May 2019

ABSTRACT

Milled banana husk, was subjected to a fast solution combustion process at different temperatures (200–900°C) to obtain ashes with determined adsorptive properties to remove radioactive pollutants from aqueous media generated by the nuclear industry. Particularly, in this work, the ashes were used to adsorb traces of ^{60}Co in presence of macro quantities of Fe(III) labeled with ^{59}Fe to follow the sorption in aqueous solution taking account the radiotoxicity of ^{60}Co and the abundance of no-radioactive Fe in the environment. For this purpose, dried banana husk (BHN) was first mixed with urea, ammonium nitrate and deionized water; then, the mixture was heated for 5 min in an oven from 200 to 900°C under standard atmospheric conditions. The obtained materials were characterized by Scanning electron microscopy (SEM), X-ray diffraction (XRD), Fourier-transform infrared spectroscopy (FT-IR), BET analysis (BET). For the sorption experimentation, the ashes samples were in contact with ^{60}Co in traces levels and Fe(III)-^{59}Fe aqueous solutions (300 or 700 mg/L). The mixtures were shaken and centrifuged to separate the phases. The ^{60}Co and ^{59}Fe activities in the liquid were determined by using a Hyperpure Germanium detector and selecting the 1.173 MeV and 1.099 MeV energies, respectively. It was found that the ash obtained at 900°C showed the highest adsorption for ^{60}Co (1.43 mg/g) in the presence of 300 ppm of Fe(III)-^{59}Fe. This ash sample presents the highest specific surface area and contains sylvite, calicinite and dolomite as the principal mineral components. The chemical species of iron could be involved as a carrier for ^{60}Co in the sorption process.

Keywords: ^{60}Co; Fe(III); ^{59}Fe; Banana-husk; Ash; Sorption

1. Introduction

Laboratory analyses of the radioactive pollutants discharged from the nuclear power stations have shown that ^{137}Cs, ^{131}I, and ^{60}Co, among others [1], are radionuclides that may have an impact on the general population. In the case of ^{137}Cs and ^{60}Co, they have relatively long half-lives and may be present in trace amounts in the environment. Traces of radionuclides dispersed into the environment during the normal operation of nuclear facilities may contribute some radiation exposure to the population. Therefore there is a demand to separate traces of radionuclides such as ^{60}Co dispersed mainly into water bodies to eliminate that exposure. Furthermore, Co is part of cobalamin, e. i. vitamin B_{12}; however in high concentration it becomes a pollutant and has been classified as a possible carcinogenic element by the IARC [2]. Rashad et al. [3] used clays (bentonite, diatomite, and sepiolite) as low-cost adsorbents for removal of Co(II) radionuclides. They found a great effect of the solution pH and the initial concentration (C_o) on Co(II) adsorption. The thermodynamic parameters ($\Delta G°$, $\Delta H°$, and $\Delta S°$) were calculated and the results showed that the present adsorption processes are feasible, spontaneous and endothermic

*Corresponding author.

in nature. Caron et al. [4] determined the behavior of ^{60}Co and ^{137}Cs by size fractionation using ultrafiltration for contaminant removal and found that the contaminant concentrations varied significantly for both contaminants in two samples taken in 2002 and 2004 (34.5 and 25.5 Bq/L for ^{60}Co, 25.5 and 97.2 Bq/L for ^{137}Cs). They also found that the size fractionation (5,000 Daa nominal cut-off) remained consistent between the 2002 and 2004 samples, as most of the ^{60}Co (72%–83%) remained in the filtrate, while almost all of the ^{137}Cs (>98%) was retained along with the colloidal-sized material.

Carbon materials have also been used as an adsorbent to separate Co from aqueous solutions. For instance, Metwally et al. [5] used egg shell material as low-cost and non-contaminant biosorbent for removal of ^{134}Cs, ^{60}Co, and $^{152+154}$Eu radionuclides from aqueous solution. The egg shell material was calcined at 500 and 800°C, and then characterized. It was found that the uptake by calcined egg shell is in the order: Eu(III) > Co(II) > Cs(I). Li et al. [6] studied the effect of pH, temperature and solution concentration on the uptake of ^{60}Co by the fungi *Paecilomyces catenlannulatus* by batch technique. The results showed that the uptake of ^{60}Co by *P. catenlannulatus* was independent of pH at pH < 5.0, whereas the enhanced uptake of ^{60}Co was observed with increasing pH from 5.0 to 8.0. The authors also found that the adsorption isotherms can be fitted by the Langmuir model very well and that the thermodynamic data indicated that the uptake process of ^{60}Co by *P. catenlannulatus* was an endothermic and spontaneous process. Other materials used to search the separation of ^{60}Co traces from aqueous solutions are Mg-Ln layered double hydroxides [7,8], antimony oxide [9], zirconium vanadate [10], microcrystalline naphthalene [11]. In addition to adsorption [5,6], ion exchange [9], coprecipitation [12] and microfiltration [13] methods have also been used to separate ^{60}Co from aqueous solutions.

Iron exists in two forms, soluble ferrous ion (Fe^{2+}) and insoluble ferric ion (Fe^{3+}). Ferrous ion can be oxidized to ferric ion (Fe^{3+}) due to the pH and dissolved oxygen in water [14,15]. Fe (II) and Co (II) may be occurring together in groundwater, but the concentration of cobalt is found to be usually much lower than the concentration of iron. The presence of iron and cobalt in water may be attributed to water percolating through soil and rock which can dissolve minerals containing iron and cobalt and hold them in water. The problems caused by Fe are not only aesthetic problems; furthermore, indirect health concerns and economic issues are other implications [15]. There are secondary standards set to constrain the emissions of iron and cobalt in the environment. The secondary standard maximum contaminant levels (MCLs) for iron and cobalt are 0.3 mg/L and 0.040 mg/L, respectively [16,17]. Therefore, it becomes necessary to remove these heavy metals from wastewaters by an appropriate treatment technology before releasing them into the environment.

Thus, in this paper ashes obtained by aqueous combustion of the banana husk at different temperatures were the adsorbents to investigate the behavior of ^{60}Co-traces in presence of macro quantities of Fe(III)-^{59}Fe to remove them from aqueous solutions considering the textural characteristics and the mineral composition of each obtained ash, as well as the chemical speciation of the Co and Fe(III) in solution.

2. Materials and methods

2.1. Materials

The banana fruit was purchased from the market of Ocoyoacac municipality, State of Mexico, Mexico. The husk was removed from the banana fruit. The banana husk was first washed with distilled water to remove dust and then dried at 353 K for 5 h. This sample was pulverized with the help of an Agatha mortar. This sample was referred as to BHN.

2.2. Thermal treatment of banana husk

One point two grams (1.2 g) of dried banana husk (BHN) were first mixed with urea (3 g), NH_4NO_3 (1.5 g) and deionized water (6 mL); then, the mixture was heated for 5 min in an oven at 200, 400, 600, 700, 800, and 900°C under standard atmospheric conditions. The obtained materials were referred as AshBH200, AshBH400, AshBH600, AshBH700, AshBH800 and Ash900, and all these samples as AshBH. AshBH samples obtained at 600–900°C were dry solids and were ground with an agate mortar; while the AshBH samples obtained at 200 and 400°C had a gummy consistency, were discarded as they could not be dried and not ground, either.

2.3. Characterization of ash samples

2.3.1. Scanning electron microscopy (SEM)

The obtained ashes were mounted directly onto scanning electron microscopy samples holders. The images were observed at 20 KeV with a Phillips XL30 electron microscopy. Elemental chemical analyses of the materials were carried out using energy X-ray dispersive spectroscopy (EDS) with a DX-4 probe.

2.3.2. X-ray diffraction (XRD)

Samples of each compound under investigation were characterized using XRD in a Siemens D5000 diffractometer with Cu Ka radiation and a diffracted beam monochromator. The X-ray tube was operated at 35 kV and 20 mA. Crystalline compounds were conventionally identified with the Joint Committee of the Powder Diffraction Standard (JPDS) cards.

2.3.3. Fourier-transform infrared spectroscopy (FT-IR)

Infrared (IR) spectra were recorded in the 4000–400 cm^{-1} range for all of the samples BHN and AshBH, using a Nicolet Magna-IR 550 FT-IR. Samples were prepared using the standard KBr pellets method.

2.3.4. BET analysis (BET)

Specific surface areas and total pore volume of solid samples were determined using the N_2 Brunauer-Emmett-Teller (BET) method. The analyser BELSORP-28SA was used for this purpose. Before the analyses, the samples were dried and degassed.

2.4. Cobalt and iron solutions

2.4.1. ^{60}Co and ^{59}Fe radioactive solutions

$Co(NO_3)_2 \cdot 6H_2O$ (0.015 g Co/mL) and $Fe(NO_3)_3 \cdot 9H_2O$ (0.1 g Fe/mL) in aqueous solutions were irradiated in a TRIGA MARK III nuclear reactor with a neutron flux of 1x 10^{12} n/cm^2 s during 2 h to obtain ^{60}Co and ^{59}Fe radionuclides.

2.4.2. Fe(III) non-radioactive solutions

Fe(III) aqueous solutions with concentrations of 200 and 600 ppm were prepared by dissolving appropriate amounts of $Fe(NO_3)_3 \cdot 9H_2O$ in 500 mL of distilled water at pH value of 5.5.

2.4.3. Fe(III) solutions labeled with ^{59}Fe

The sorption of Fe(III) from aqueous solutions by ash materials was followed with adding 10 µL of ^{59}Fe radioactive solution to 10 mL of nonradioactive Fe(III) solutions which final concentrations were 300 and 700 mg/L. This solution was named as Fe(III)-^{59}Fe.

2.5. ^{60}Co and Fe(III)-^{59}Fe sorption

One hundred milligrams of AshBH samples, with 10 mL of 300 or 700 mg/L Fe(III)-^{59}Fe aqueous solutions were shaken for 24 h at 20°C in separate glass vials. Before shaking, 10 µL of the ^{60}Co irradiated aqueous solutions were added to each vial. The final concentration of ^{60}Co in the vials was 15 mg/L. After shaking, the mixture was centrifuged to separate the phases. The liquid was recovered with a pipette, and the solid was discarded. The ^{60}Co and ^{59}Fe activities in the liquid were determined by using a Hyperpure Germanium (HP-Ge ORTEC, 2012-19200) detector and selecting the 1.173 MeV and 1.099 MeV energies with a multichannel analyzer (program "Nucleus PCA II), respectively. The retention percentage was calculated using the expression; % R = $(A_r/A_s)\times100$ where A_r is the activity of ^{60}Co or ^{59}Fe in the remained solutions and A_s is the initial activity before the sorption processes. The experiments were performed in duplicate.

3. Results and discussion

3.1. Scanning electron microscopy (SEM) and energy X-ray dispersive spectroscopy (EDS)

Fig. 1 shows the SEM images of banana husk samples (a) washed with distilled water (BHN), (b) AshBH600, (c) AshBH700, (d) AshBH800), and (e) AshBH900. The surface texture of the BHN sample is rough and gutters were observed in it. The images of AshBH600, AshBH700, AshBH800, and AshBH900, show a noticeable porosity due to the obtention of the materials by a liquid combustion process. AshBH900 sample seems to be formed by the agglomeration of very small particles. This change has been observed in other types of raw materials from agriculture wastes [18,19].

The results of the elemental analyses by EDS of samples BHN, AshBH600, AshBH700, AshBH800, and AshBH900 are shown in Table 1.

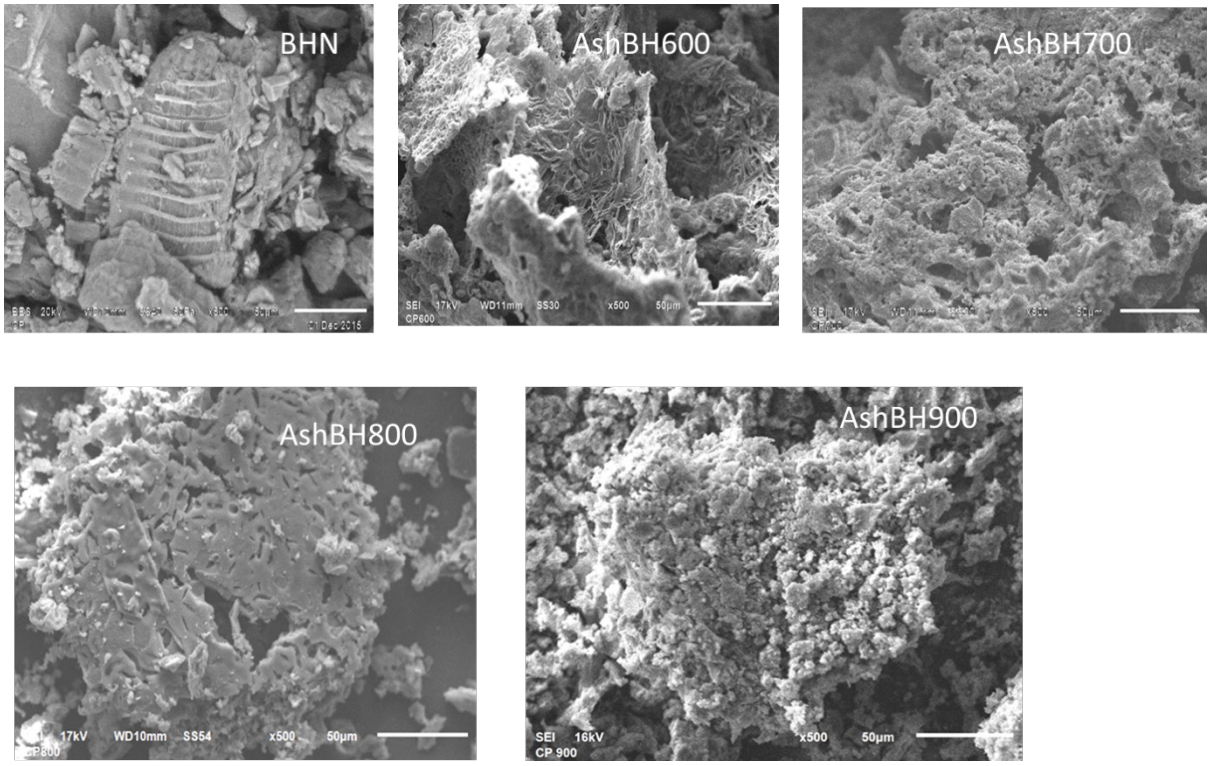

Fig. 1. SEM images of (a) BHN, (b) AshBH600, (c) AshBH700, (d) AshBH800, and (e) AshBH900.

Table 1
Elemental composition of BHN and AshBH samples obtained by chemical combustion processes

Element	Weight %				
	BHN	AshBH600	AshBH700	AshBH800	AshBH900
C	60.89±2.38	50.34±5.0	39.11±9.52	36.30±8.13	30.12±9.06
O	35.28±2.57	22.70±2.76	29.08±6.37	33.40±2.61	39.76±6.03
Mg	0.10±0.01	0.69±0.08	0.54±0.05	0.74±0.22	0.72±0.13
Cl	0.64±0.20	0.27±0.05	3.56±1.08	2.39±0.64	1.77±0.7
Si	0.39±0.25	1.22±0.52	1.64±0.53	2.40±1.67	1.33±0.32
K	2.69±0.62	22.87±4.98	25.61±5.39	23.44±5.61	25.14±5.77
P	0.16±0.04	0.67±0.37	0.27±0.01	0.48±0.00	0.8±0.04
Ca	0.05±0.03	1.31±0.11	0.55±0.05	1.84±0.73	1.77±0.3

All the AshBH samples contain C, O, Mg, Si, K, Ca and P. The C (<50 %) and O (<22 %) are the major elements in all samples followed by K and in less amount Cl, Si and Ca. It is important to mention that the amount of K in AshBH samples is 10 times higher than that of BHN.

3.1.2. X-ray diffraction (XRD)

Fig. 2 shows X-ray diffraction (XRD) patterns of BHN, AshBH600, AshBH700, AshBH800, and AshBH900 samples, respectively. The BHN sample shows a reflexion at 20 2-theta degrees. This broad reflexion has been attributed to cellulosic compounds [20,21]. The AshBH samples (Fig. 2) show broad peaks centered at 26, 28 and 30 2-theta degrees depending on the temperature used for the chemical combustion processes, thus these samples have partially an amorphous structure. As observed in the same figure, the AshBH samples also have sharp and well defined peaks which identity were proposed in Table 2.

It is important to mention that other authors have found that the calcination temperature of biomasses determines the morphology, the elemental components, the mineral composition and the textural characteristics of the obtained ashes [22–24]. The differences between those works and the present one are that the ashes were got through solution combustion process at different temperatures in a few minutes obtaining ashes with different adsorptive properties that can use for the removal (in trace level) of radioactive isotopes from water.

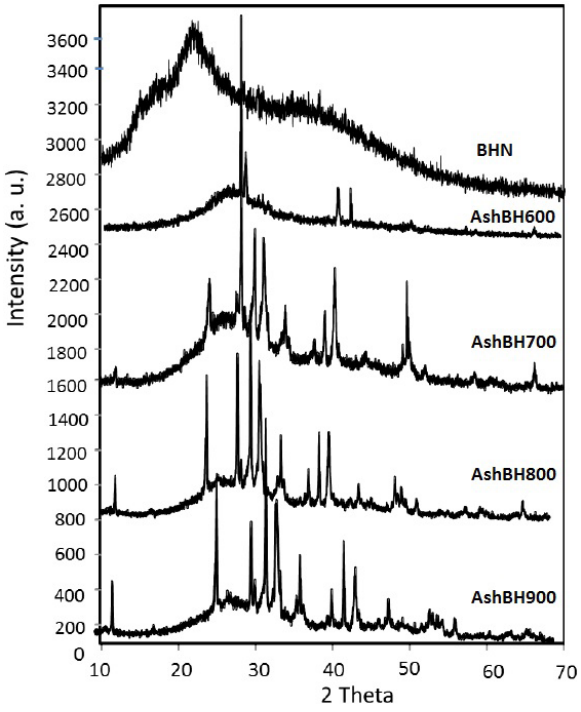

Fig. 2. X-ray diffraction patterns of (a) BHN, (b) AshBH600, (c) AshBH700, (d) AshBH800, and (e) AshBH900.

3.1.3. Fourier-transform infrared spectroscopy (FT-IR)

The main bands found in banana husk sample (Fig. 3) were assigned as follows: the intense band observed at 3440 cm^{-1} indicates the presence of OH groups in the banana husk; the wave number at 1633 cm^{-1} results from a CO stretching mode conjugated with an NH deformation and indicates the presence of an amide group. The 1059 cm^{-1} band is assigned to CO or CN groups. The band at 2305 cm^{-1} was recognized as a CO group, which may result from the presence of atmospheric CO_2.

FT-IR spectra of AShBH600, AshBH700, AshBH800, and AshBH900 are very similar (Fig. 3) and the main bands observed were recognized as follows: The most intense peak at 3430 cm^{-1} was assigned to $^{-}$OH stretching, while the

Table 2
Compounds that could be generated by the liquid combustion process of BHN at different temperatures

Sample	Compound	Name	JSPDS Card
AshBH600	KCl	Sylvite	73-0380
AshBH700	$KHCO_3$	Calicinite	70-0995
AshBH800	KCl	Sylvite	73-0380
	$KHCO_3$	Calicinite	70-0995
AshBH900	KCl	Sylvite	73-0380
	$KHCO_3$	Calicinite	70-0995
			12-0292
	$CaMg(CO_3)_2$	Dolomite	89-5862

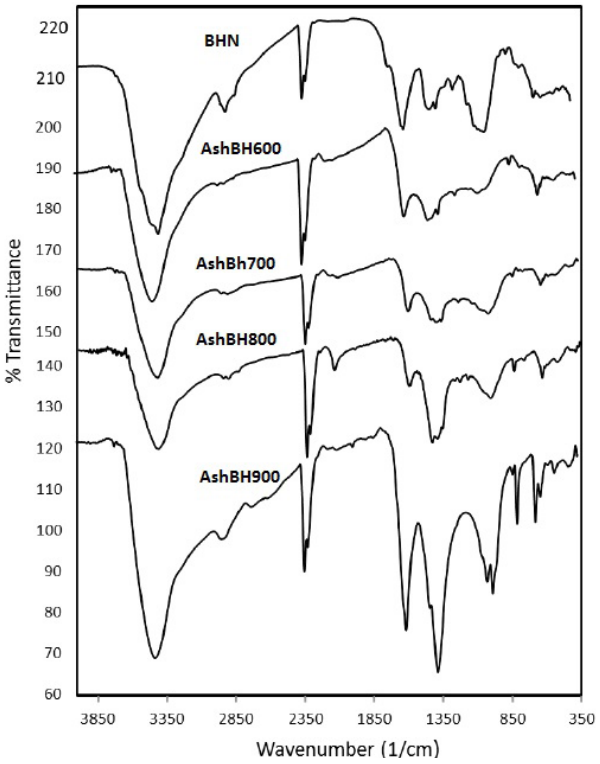

Fig. 3. FT-IR spectra of BHN, AshBH600, AshBH700, AshBH800, and AshBH700 samples.

two peaks observed at 2860 and 2998 cm $^{-1}$ may be due to symmetric and asymmetric -CH_2 stretching, respectively. The peak at 1630 cm^{-1} may be to C=C or C=O stretching or -OH bending; while the peak at 1410 cm^{-1} may be due to a bending of the O-H bond also.

3.1.4. Brunauer-Emmett-Teller analyses (BET)

Table 3 displays the specific areas, total pore volume and mean pore diameter for BHN and AshBH samples (materials obtained at 600, 700, 800, and 900°C by solution combustion of banana husk). The results show that as the combustion temperature is increased, the values of the specific surface areas are also increased up to the temperature of 900°C. This behavior is also observed for total pore volume. The pore diameter of the AshBH samples increases when the combustion temperature of the BHN increases except for the sample AshBH900.

3.2. ^{60}Co and Fe(III)-^{59}Fe sorption

3.2.1. ^{60}Co sorption in presence of Fe(III)-^{59}Fe in aqueous solutions by BHN and AshBH

The combustion process to obtain the different materials modifies the morphology (Fig. 1) and the textural characteristics of the obtained products (Table 3) at the different temperatures (600, 700, 800, and 900°C) as was mentioned earlier. These changes in the textural characteristics lead to different adsorption efficiencies to remove ^{60}Co from aqueous solutions.

Table 3
Textural parameters for BHN, and of the obtained carbon by chemical combustion processes (AshBH)

Sample	Specific surface area (cm^2/g)	Total pore volume (cm^3/g)	Pore diameter (nm)
BHN	0.46	0.0010	9.2
AshBH600	2.30	0.0066	13.8
AshBH700	3.84	0.0121	30.4
AshBH800	4.91	0.0160	36.8
AshBH900	18.82	0.0319	5.3

Fig. 4 shows the ^{60}Co sorption by the BHN and ash samples (AshBH) as a function of their specific surface area. ^{60}Co in the starting aqueous solution was present in trace quantities, while Fe(III) was present in macro amounts (300 ppm) labeled with ^{59}Fe to follow its adsorption process. As can be seen, ^{60}Co sorption was increased as the specific surface area was increased as well from 0.46 to 18.82, finding that the maximum ^{60}Co sorption was 1.43 mg/g for AshBH900 which has the biggest specific surface area with respect the others materials. At the lowest combustion temperature (600°C, corresponding to sample AshBH600 with a specific surface area of 2.30 cm^2/g) the ^{60}Co sorption notably diminishes. Slightly adsorption of ^{60}Co was observed for the banana husk before combustion (BHN).

In the same Fig. 4 the ^{60}Co sorption by the BHN and ash materials as a function of their specific surface area is displayed considering now a Fe(III)-^{59}Fe concentration of 700 ppm while ^{60}Co was used again in traces amounts. The results show that the ^{60}Co sorption was increased rapidly from the ash materials obtained from 600°C to 800°C which specific surface areas correspond to 2.30 and 4.91 cm^2/g, respectively. Then it remained practically constant reaching a sorption capacity around 0.54 mg/g. It is important to mention that when the ^{60}Co-traces are in a Fe(III)-^{59}Fe solution of 700 ppm, the sorption by the AshBH 900 diminishes 62% with respects to that of 300 ppm. This behavior can be explained by the saturation of the ashes surface by Fe(III)-^{59}Fe that avoid the interaction with the ^{60}Co.

3.2.2. Fe(III)-^{59}Fe sorption by BHN and AshBH in presence of ^{60}Co-traces in aqueous solutions

Fig. 5 shows the sorption of Fe(III)-^{59}Fe in presence of ^{60}Co-traces by the ash materials obtained at 600, 700, 800 and 900°C using the solution combustion process of banana husk. The concentrations of Fe(III)-^{59}Fe in the aqueous solution in contact with the ash materials were 300 and 700 ppm, as was mentioned before. As can be seen, the sorption capacities of the AshBH depends on the initial concentration of Fe(III)-^{59}Fe in solution. When the initial concentration is high the sorption of Fe(III)-^{59}Fe is high as well. The specific surface areas of the BHN and ash materials influence on the sorption behavior. When they increase from 2.30 to 4.91 cm^2/g the sorption goes increased from 8.12 to 27.09 mg/g for a solution of 300 ppm of Fe(III)-^{59}Fe and from 19.61 to 70.00 mg/g for a solution of 700 ppm.

A particular behavior was observed for AshBH900, which have the highest specific surface area (18.82 cm^2/g),

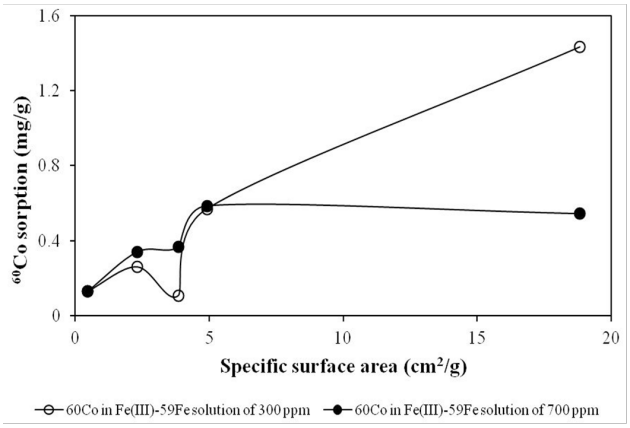

Fig. 4. ^{60}Co sorption in the presence of Fe(III)-^{59}Fe (300 and 700 ppm) by BHN and AshBH as a function of their specific surface areas.

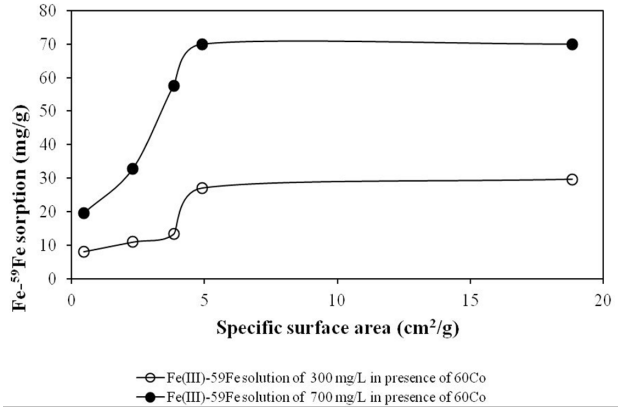

Fig. 5. Fe(III)-^{59}Fe sorption in the presence of ^{60}Co traces by BHN and AshBH as a function of their specific surface areas and Fe concentrations in aqueous solution of 300 and 700 ppm.

after contact with a Fe(III)-^{59}Fe solution of 300 and 700 ppm because in these cases similar sorption capacities were found (29.71 and 70.00 mg/g, respectively) with respect to the sample AshBH800 with a specific surface area of 4.91 cm^2/g. This result can be explained with base on the pore diameter (Table 3) which was diminished drastically for effect of the temperature to obtain ashes from banana husk at 900°C.

3.2.3. Linear model

The obtained data were fitted to the linear model to compare the results in the different experimental conditions. For this purpose, in general, it was considered the specific surface areas from 0.46 to 4.91 cm^2/g and the corresponding sorption capacities of the BHN and AshBH materials for ^{60}Co and Fe(III)-^{59}Fe, where the observed behavior maintained a proportionality and a plateau was not observed.

As can be noticed in Fig. 6, the ^{60}Co sorption by BHN, AshBH600, AshBH700, AshBH800, and AshBH900 has a linear behavior considering their specific surface area (Table 3) and a Fe(III)-^{59}Fe concentration of 300 ppm. Similar behavior was observed when the concentration of Fe increases for 300 to 700 ppm and the specific surface areas of the materials vary from 0.46 to 4.91 cm^2/g, except for the highest specific surface area. When the specific surface area increases at 18.82 cm^2/g the amount of ^{60}Co is similar to that found at 4.91 cm^2/g (Fig. 6). The slope of the curves, which represent the amount of ^{60}Co sorbed on the surface area of the materials, varies between 300 and 700 ppm. In the first case was 0.0729 mg/cm^2 and in the second one was 0.0917 mg/cm^2 (the determination parameter was higher than 0.91). The highest concentration of Fe in solution slightly improved 1–3 times the ratio between the ^{60}Co sorption and the specific surface area of each material into the interval of 0.46 and 4.91 cm^2/g. It is important to emphasize that ^{60}Co was in a trace level with respect the concentration of Fe(III)-^{59}Fe in the solution.

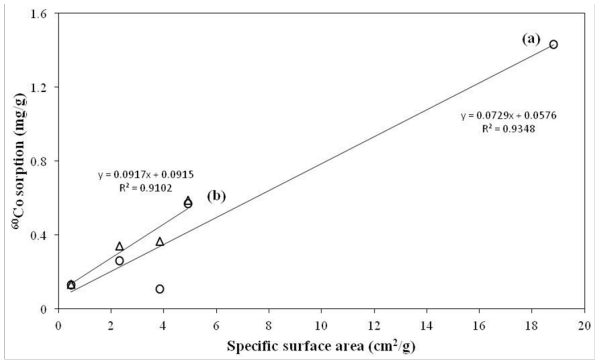

Fig. 6. Linear model applied to the ^{60}Co sorption by BHN and AshBH considering their specific surface areas and Fe concentrations of 300 ppm (a) and 700 ppm (b).

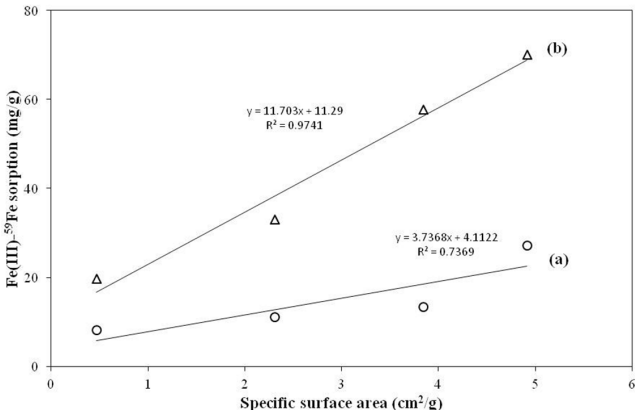

Fig. 7. Linear model applied to the Fe(III)-^{59}Fe sorption by BHN and AshBH considering their specific surface areas and Fe concentrations of 300 ppm (a) and 700 ppm (b).

Fig. 7 shows that the Fe(III)-^{59}Fe sorption by BHN, AshBH600, AshBH700 and AshBH800 also has a linear behavior in similar form than ^{60}Co, with base on their specific surface areas (Table 3), for both Fe concentration in solution. The slope of the curves varies considerably between 300 and 700 ppm which were 3.7368 mg/cm^2 and 11.7030 mg/cm^2 (the determination parameter was higher than 0.73). The concentration of Fe in solution improved 2 and 4

times the ratio between the Fe(III)-^{59}Fe sorption depending on the specific surface area of each material. This difference is similar to that found for ^{60}Co although this radionuclide was in a trace level in solution with respect to Fe(III)-^{59}Fe. With base on this behavior it is reasonable to propose that Fe(III)-^{59}Fe could function as a carrier of ^{60}Co [25] and additionally the chemical speciation of Fe(III) (Fe_2O_3 at pH from 2 to 12) and Co(II) (Co^{2+} at pH < 6.5) could play a role in the sorption processes [26].

4. Conclusions

Milled banana husk is modified by the aqueous solution combustion process from 600 to 900°C in a brief period (5 min) changing the morphology, elemental composition, mineral components and the surface area (from 0.46 up to 18.82 cm^2/g) of the obtained ash materials. The highest sorption capacities for ^{60}Co in the presence of 300 and 700 ppm of Fe(III)-^{59}Fe by the AshBH900 are 1.43 mg/g and 0.54 mg/g, respectively, while for Fe(III)-^{59}Fe in presence of trace of ^{60}Co are 29.71 mg/g and 70.0 mg/g, respectively. The AshBH800 shows the maximum adsorption capacity for Fe(III)-^{59}Fe which is 70 mg/g. The sorption capacity of the ash material obtained from milled banana husk by aqueous combustion is in function of the material surface properties and the chemical speciation of ^{60}Co and Fe(III)-^{59}Fe in the aqueous media. The AshBH are materials to adsorb both ^{60}Co and Fe(III)-^{59}Fe from bi-component solutions. The Fe(III)-^{59}Fe can be a carrier of ^{60}Co to be adsorbed by the ash materials.

Acknowledgments

Authors thank CONACyT (project 254665) for the financial support of this research. The authors are grateful for the contributions of J. Serrano-Gómez to this manuscript.

References

[1] S.H. Sheen, Detection and monitoring of leaks at nuclear power plants external to structures, Argonne National Laboratories, US, 2012. ANL/NE-12/32.
[2] IARC, International Agency for Research in Cancer, Cobalt and cobalt compounds, Lyon, France, 1991.
[3] G.M. Rashad, M.R. Mahmoud, A.M. Elewa, E. Merwally, E.A. Saad, Removal of radiocobalt from aqueous solutions by adsorption onto low-cost adsorbents, J. Radioanal. Nucl. Ch., 309 (2016) 1065–1076.
[4] F. Caron, S. Laurin, C. Simister, C. Jacques, G. Mankarios, Potential use of ultrafiltration for groundwater remediation and aqueous speciation of Co-60 and Cs-137 from a Contaminated Area, Water Air Soil Poll., 178 (2007) 121–130.
[5] S.S. Metwally, R.R. Ayoub, H.F. Aly, Utilization of low cost sorbent for removal and separation of ^{134}Cs, ^{60}Co and $^{152+154}$Eu radionuclides from aqueous solution, J. Radioanal. Nucl. Ch., 302 (2014) 441–449.
[6] F. Li, Z. Gao, X. Li, L. Fang, The effect of environmental factor on the uptake of ^{60}Co by Paecilomyces catenlannulatus, J. Radioanal. Nucl. Ch., 299 (2014)1281–1286.
[7] S.A. Kulyukhin, E.P. Krasavina, I.A. Rumer, Separation of ^{60}Co, ^{90}Sr, ^{90}Y and ^{137}Cs from aqueous solutions onto Mg-Ln layered double hydroxides (Ln = Ce, Pr, Sm, Gd), Radiochemistry, 55 (2013) 596–600.
[8] S.A. Kulyukhin, E.P. Krasavina, I.A. Rumer, I.V. Klimovivh, Sorption of ^{60}Co from aqueous solutions onto layered double hydroxides of various compositions, Radiochemistry, 57 (2015) 152–160.
[9] L. Malinen, R. Koivula, R. Harjula, Removal of cobalt from aqueous solutions containing EDTA under UV-C irradiation by antimony oxide, Radiochim. Acta, 104 (2016) 415–422.
[10] A.M.H Ibrahim, I.M. Ali, E.S. Zakaria, I.M. El-Naggar, Adsorption and kinetic performance of Cs^+, Co^{2+}, and Ce^{4+} radionuclides on zirconium vanadate as a cation exchanger, Radiochemistry, 55 (2013) 581–588.
[11] H.M. Mohamed, A.M. Fatty, M.S. Sayed, Simultaneous solid phase extraction of cobalt, strontium and cesium from liquid radioactive waste using microcrystalline naphthalene, Radiochim. Acta, 102 (2014) 1017–1024.
[12] S.A. Kulyukhin, M.P. Gorvacheva, I.A. Rumer, Coprecipitation of ^{60}Co with *d* element sulfides from aqueous solutions in the presence of EDTA, Radiochemistry, 56 (2014) 19–21.
[13] V.V. Milyutin, N.A. Nekrasova, V.O. Kaptakov, Removal of radionuclide and corrosion products from neutral and weakly alkaline solutions by microfiltration, Radiochemistry, 58 (2016) 30–33.
[14] N. Ahalya, R.D. Kanamadi, T.V. Ramachandra, Biosorption of iron(III) from aqueous solutions using the husk of Cicer arientinum, Indian J. Chem. Techn., 13 (2006) 122–127.
[15] Y. Zhang, J. Zhao, Z. Jiang, D. Shan, Y. Lu, Biosorption of Fe(II) and Mn(II) ions from aqueous solution by rice husk ash, Biomed. Res. Int., (2014) 973095.
[16] R.E.R. Machmeier, Iron and Drinking Water, AG-FO, 1318, University of Minnesota, US, 1990.
[17] WI DNR-Drinking water and groundwater quality standars/advisory levels, Wisconsin Department of Natural Resources, US, 2011.
[18] J. Serrano-Gómez, H. López-González, M.T. Olguin, S. Bulbulian, Carbonaceous material obtained from exhausted coffee by an aqueous solution combustion process and used for cobalt (II) and cadmium (II) sorption, J. Environ. Manage., 156 (2015) 121–127.
[19] H. López-González, J. Serrano-Gómez, M.T. Olguin, J. Hernández-López, S. Bulbulian, Removal of Co by carbonaceous material obtained through solution combustion of tamarind shell, Int. J. Phytoremediat., 19 (2017) 1126–1133.
[20] C. Djilani, R. Zaghdoudi, A. Modarressi, M. Rogalski, F. Djazi, A. Lallam, Elimination of organic micropollutants by adsorption on activated carbon prepared from agricultura waste, Chem. Eng. J., 189 (2012) 203–212.
[21] C. Qin, Y. Chen, J.M. Gaon, Manufacture and characterization of activated carbon from marigold Straw (Tagetes erecta L) by H_3PO_4 chemical activation, Mater. Lett., 135 (2014) 123–126.
[22] X. Yao, K. Xu, Comparative study of characterization and utilization of corncob ashes from gasification process and combustion process, Constr. Build. Mater., 119 (2016) 215–222.
[23] E. Romero, M. Quirantes, R. Nogales, Characterization of biomass ashes produced at different temperatures from olive-oil-industry and greenhouse vegetable wastes, Fuel, 208 (2017) 1–9.
[24] X. Yao, K. Xu, F. Yang, Y. Liang, The influence of ashing temperature on ash fouling and slagging characteristics during combustion of biomass fuels, Bioresources, 12 (2017) 1593–1610.
[25] G.L. Woodward, C.L. Peacock, A. Otero-Fariña, O.R. Thompson, A.P. Brown, I.T. Burke, A universal uptake mechanism for cobalt(II) on soil constituents: Ferrihydrite, kaolinite, humic acid, and organo-mineral composites, Geochim. Cosmochim. Ac., 238 (2018) 270–291.
[26] I. Puigdomenech, Program MEDUSA (Make Equilibrium Diagrams Using Sophisticated Algorithms), 2013.